Stem Cells Translational Medicine, 2022, **11**, 213–229
https://doi.org/10.1093/stcltm/szab021
Advance access publication 8 March 2022
Original Research

T-cadherin Expressing Cells in the Stromal Vascular Fraction of Human Adipose Tissue: Role in Osteogenesis and Angiogenesis

Julien Guerrero[1], Boris Dasen[1], Agne Frismantiene[1], Sebastien Pigeot[1], Tarek Ismail[1,2], Dirk J. Schaefer[2], Maria Philippova[1], Therese J. Resink[1], Ivan Martin[1], Arnaud Scherberich[1,2]*

[1]Department of Biomedicine, University Hospital Basel, University of Basel, Basel, Switzerland
[2]Department of Plastic, Reconstructive, Aesthetic and Hand Surgery, University Hospital Basel, Basel, Switzerland

*Corresponding author: Arnaud Scherberich, Department of Biomedicine, Hebelstrasse 20, University Hospital Basel, 4031 Basel, Switzerland. Tel: +41 061 328 73 75; Email: arnaud.scherberich@usb.ch

Abstract

Cells of the stromal vascular fraction (SVF) of human adipose tissue have the capacity to generate osteogenic grafts with intrinsic vasculogenic properties. However, cultured adipose-derived stromal cells (ASCs), even after minimal monolayer expansion, lose osteogenic capacity in vivo. Communication between endothelial and stromal/mesenchymal cell lineages has been suggested to improve bone formation and vascularization by engineered tissues. Here, we investigated the specific role of a subpopulation of SVF cells positive for T-cadherin (T-cad), a putative endothelial marker. We found that maintenance during monolayer expansion of a T-cad-positive cell population, composed of endothelial lineage cells (ECs), is mandatory to preserve the osteogenic capacity of SVF cells in vivo and strongly supports their vasculogenic properties. Depletion of T-cad-positive cells from the SVF totally impaired bone formation in vivo and strongly reduced vascularization by SVF cells in association with decreased VEGF and Adiponectin expression. The osteogenic potential of T-cad-depleted SVF cells was fully rescued by co-culture with ECs from a human umbilical vein (HUVECs), constitutively expressing T-cad. Ectopic expression of T-cad in ASCs stimulated mineralization in vitro but failed to rescue osteogenic potential in vivo, indicating that the endothelial nature of the T-cad-positive cells is the key factor for induction of osteogenesis in engineered grafts based on SVF cells. This study demonstrates that crosstalk between stromal and T-cad expressing endothelial cells within adipose tissue critically regulates osteogenesis, with VEGF and adiponectin as associated molecular mediators.

Key words: adipose stem cells; 3D microenvironment; bone; blood vessels; osteogenesis; angiogenesis.

Graphical Abstract

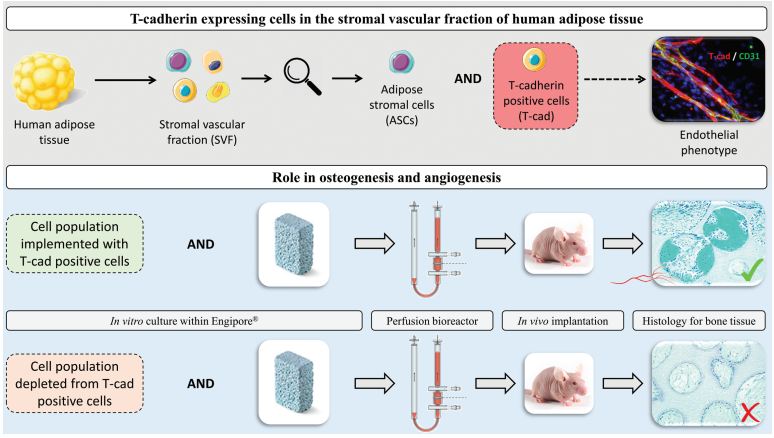

Significance Statement

The crosstalk between endothelial cell and stromal cells is critical in osteogenesis. In this study we demonstrate that a cell subpopulation from the stromal vascular fraction of human adipose tissue, namely T-cadherin-positive cells with endothelial cell identity, supports a better performance both in terms of osteogenic and angiogenic differentiation as compared to expanded adipose stromal cells which mostly lack this population. This project not only has a scientific impact by evaluating the role of this T-cadherin positive population on bone formation and vasculogenesis but could also lead to an innovative clinical approach with cell therapy for bone tissue regeneration.

Received: 11 June 2021; Accepted: 31 October 2021.

Introduction

In the field of bone tissue regeneration, a large number of studies have examined the osteogenic potential of human mesenchymal stromal cells from various sources, possibly combined with 3-dimensional (3D) matrices or biomaterials as cell carriers. However, vascularization remains one of the main hurdles in the reconstruction of large bone defects.[1] Insufficient vascularization after implantation of tissue-engineered constructs with stromal cells leads to nutrient limitation, resulting in cell death within the constructs.[2,3] Several strategies for improving vascularization and engraftment of tissue-engineered constructs have been proposed.[4] The freshly isolated stromal vascular fraction (SVF) of human adipose tissue contains not only mesenchymal/stromal progenitors but also cells with vasculogenic phenotype.[5] Freshly isolated SVF cells can generate bone and functional blood vessels in vivo if suitably induced by 3D culture under perfusion flow[6] or osteo-inductive triggers.[7]

Following culture expansion, adipose-derived stromal cells (ASCs) are a promising cell source for bone reconstruction and regeneration.[8-10] Even if ASCs were recently documented as inferior in the ability to induce bone formation in vivo in comparison to bone marrow-derived mesenchymal stromal cells (BMSCs),[11] many in vitro and in vivo models suggest that the use of ASCs, provided suitable priming in culture, can improve bone healing through direct differentiation into osteoblasts as well as paracrine effects that facilitate migration and differentiation of resident precursors.[12-15] Indeed, it is well described that the secretomes of SVF cells[16,17] and of expanded ASCs[18,19] are rich in growth factors, angiogenic cytokines, adipokines, and neurotrophic factors involved in bone homeostatic processes.[20-22] Bone formation and engraftment of tissue-engineered constructs can be improved by supplementation with ECs, their progenitors, or endothelial growth factors, especially in the context of critically sized grafts.[23-28] Moreover, it was recently shown that endothelial cells play a crucial role through the paracrine effect in bone formation.[29] There is evidence that the processes of angiogenesis and osteogenesis strongly depend on a tight interaction between bone-forming cells and endothelial/vascular cells.[30-32]

In vitro studies have shown that cells of endothelial/mesenchymal lineages present within the SVF isolated from adipose tissue contribute to the formation of a vascular network organized as tube-like structures and to osteogenesis.[33,34] In vivo, implantation of tissue-engineered constructs seeded with SVF cells leads to the formation of a bone/osteoid tissue exhibiting numerous vessels,[35,36] although the underlying mechanism remains largely unknown. Importantly, however, SVF cells lose their osteogenic capacity even after minimal monolayer expansion.[6] One hypothesis concerning the loss of osteogenic potential is that culture and expansion of stromal/stem cells in vitro induces phenotypic alterations that diminish their osteogenic capacity in vivo.[6,37] An alternative hypothesis is that a reduction in the proportion of endothelial progenitor cells after monolayer expansion of SVF cells can negatively affect the osteogenic differentiation potential of ASCs. In the context of bone-tissue engineering, the relevance of paracrine communication between osteogenic and endothelial cell lineages has long been recognized.[26] However, interactions between endothelial and stromal compartments have not been studied in SVF cells.

Cadherins are a superfamily of integral transmembrane proteins that mediate calcium-dependent cell-cell adhesion. Bone forming cells express multiple cadherins such as N-cadherin[38] and cadherin-11.[39] It was already shown that upregulation of N-cadherin and cadherin-11 parallels osteogenic cell differentiation of mesenchymal precursors.[40,41] Another member of this superfamily, T-cadherin (T-cad/CDH13), is a cell surface protein, with 2 described isoforms.[42] It is expressed in the aorta, carotid, iliac, renal arteries, capillaries, and the heart and is present on endothelial cells (ECs), pericytes, vascular smooth muscle cells, and cardiomyocytes. T-cad is a recognized regulator of EC function.[43,44] In vitro expression of T-cad on ECs is upregulated during proliferation and oxidative or endoplasmic reticulum stress.[45,46] In vivo expression of T-cad on ECs increases in human atherosclerotic lesions[45] and experimental restenosis.[47] Together, these observations strongly suggest the involvement of T-cad in vascular function and remodeling. Clinical evidence supports an association between T-cad and hypoadiponectinemia, with an increased risk of various metabolic diseases,[48,49] while a study in lean and obese mouse models suggests also a role for T-cad in adipose tissue health.[50] T-cadherin plays an essential role in the binding of adiponectin to ECs and its functional effects in the vessel.[51] However, no direct study of T-cad in human adipose tissue, and more specifically in the SVF multicellular population, is available.

The goal of the present work is (1) to investigate the presence of T-cad-positive cells as endothelial component within SVF from human adipose tissue and (2) to examine their impact on the osteogenic and vasculogenic potential of SVF cells and ASCs both in vitro during 2D monolayer culture and in vivo following 3D scaffold culture and implantation. Our findings support that T-cad expressing cells present in the SVF fraction of human adipose tissue play a critical role in the bone and vascular potential of this stromal fraction. A better understanding of cell interactions between stromal and endothelial compartments in SVF is an important step toward developing tissue-engineering strategies that reliably support bone and vasculature formation.

Materials and Methods

Cell Isolation

Subcutaneous adipose tissue in the form of lipoaspirates or excision fat was obtained from 20 healthy donors during routine liposuctions, after informed consent from the patient and following protocol approval by the ethical committee of the local Government (Permit number 78/07 of the Ethikkommission beider Basel, Kanton Basel-Stadt, Basel, Switzerland). All the methods were conducted in accordance with the relevant guidelines and regulations. The tissue was digested in 0.075% collagenase type 2 (#LS004176, Worthington) for 45 minutes at 37°C on an orbital shaker. The suspension was centrifuged at 300 *g* for 10 minutes, and the resulting stromal vascular fraction (SVF) pellet was rinsed once with phosphate-buffered saline (PBS, #10010023 Gibco), suspended in alpha-minimal essential medium (α-MEM, #12571063, Gibco) and filtered through a 100 μm strainer (#352360, BD Falcon). Nucleated cells were counted after staining with 0.01% Crystal Violet (#V5265, Sigma) in PBS.

Cell Culture

For cell expansion, freshly isolated SVF cells were plated at a density of 1×10^5 cells/cm^2. When confluency was achieved, one part of the cells were either detached with 0.05%

trypsin/0.01% EDTA (#25300054, Gibco) and re-plated at a density of 1 × 10^5 cells/cm^2 (ASCs). The other part of the cells was further cultured without passaging for 28 days (Unpass cells). Cells were cultured in complete medium (CM), consisting of alpha-minimal essential medium (α-MEM, #12571063, Gibco) supplemented with 10% fetal bovine serum (FBS, #16000044, Gibco), 1% HEPES (#15630080, Gibco), 1% sodium pyruvate (#11360070, Gibco), and 1% penicillin-streptomycin-glutamine (PSG, #10378016, Gibco) solution, supplemented with 5 ng/mL fibroblast growth factor-2 (FGF-2, #233-FB,R&D systems) and filtered through a 100 µm strainer (#352360, BD Falcon). Human umbilical vein endothelial cells (HUVECs) (#C-12200, PromoCell) were cultured on 2% gelatin-coated plates directly after thawing, within CM medium also supplemented with 5 ng/mL FGF-2. Cells were cultured at 37°C in a 5% CO_2 with a 95% air-humidified incubator.

Western Blot

Cells were rinsed with PBS and lysed in lysis buffer (RIPA, # 89900, Thermo Fischer Scientific) containing 25 mM Tris-HCl (pH 7.4), 150 mM NaCl, 1% NP-40, 1 mM EDTA, 5% glycerol, with the inclusion of phosphatase inhibitor cocktail and protease inhibitor cocktail (#78440, Thermo Fischer Scientific). Protein concentrations were determined using the BCA Protein Assay Kit (#23225, Thermo Fischer Scientific). Crude cell protein lysates (10 µg/lane) were subjected to standard SDS-polyacrylamide gel electrophoresis under reducing conditions and electro-blotted onto nitrocellulose. Membranes were immuno-probed using primary antibodies against T-cad at 1:100 (#SAB1408557, Sigma), with β-actin at 1:500 (#ab8229) and GAPDH at 1:2500 (#ab9485, Abcam) as the internal protein loading control. Secondary HRP-conjugated anti-species-specific IgGs (used at 1:2000) were from Southern Biotechnology (#4090-05, BioReba). Immunoreactive proteins were detected using Pierce ECL Western blotting substrate (#32106, Thermo Fischer Scientific) with signal capture using the Bio-Rad Molecular Imager Gel Doc XR+ system (Bio-Rad). Signal intensities were quantified using Image J software, and to correct for variations in sample loading T-cad values were normalized with respect to their corresponding β-actin and GAPDH values.

Immunofluorescence Staining

After 28 days of culture, Unpass cells were fixed with 1% PFA for 1 hour and washed twice with PBS. For human native adipose tissue, samples were fixed overnight with 1% PFA and washed twice with PBS, embedded in paraffin wax, and sectioned (7 µm). Antibodies against T-cad at 1:100 (#ABT121, Sigma), vWF at 1:500 (#M0616, Dako), CD31 at 1:250 (#MA5-13188, Invitrogen), and Laminin at 1:250 (#33-530, Invitrogen) were used as primary antibodies. Fluorescent-conjugated secondary antibodies chicken anti-rabbit Alexa 488 (#A-21441, Thermo Fischer Scientific) and goat anti-mouse Alexa 546 (#A-11030, Thermo Fischer Scientific) were both used at 1:500. Images were acquired with a Nikon A1R confocal microscope.

Cell Sorting

Cells (3-5 × 10^6 cells) were suspended in 1000 µL of 0.5% BSA in PBS (fluorescence-activated cell sorting; FACS buffer). For sorting experiments, freshly isolated SVF cells or Unpass cells were stained for 30 minutes at 4°C with antibodies specific for T-cad at 1:100 (#ABT121, Sigma) or an isotype control at 1:100 (#269A-1, Sigma), and a secondary antibody conjugated with chicken anti-rabbit Alexa 488 at 1:250 (#A-21441, Thermo Fischer Scientific), in 0.5% BSA in PBS. The T-cad-positive cell population was then sorted out with a FACS-Vantage SE cell sorter (Becton, Dickinson and Company). The gating strategy is shown in Supplementary Fig. 1.

Real-time PCR

Total RNA was extracted from cells for each condition with the RNeasy Mini kit protocol (Qiagen). All RNAs were treated by Deoxyribonuclease I (DNAse I; Invitrogen), and total RNA was reverse-transcribed into cDNA with the Omniscript Reverse Transcription kit (Qiagen) at 37°C for 60 minutes. Quantitative real-time PCR assays were performed with ABIPrism 77000 Sequence Detection System (Perkin Elmer/Applied Biosystem, Rotkreuz) and utilizing Taqman Universal PCR Master Mix (Applied Biosystems). The cycling parameters were the following: 50°C for 2 minutes, followed by 95°C for 10 minutes and 40 cycles of denaturation at 95°C for 15 seconds and annealing/extension at 60°C for 1 minute. Reactions were performed in triplicate for each template and specific gene expression was evaluated using the 2ΔΔCT method. Gene expression levels were normalized to the GAPDH mRNA as previously described.[52] Primers and probes for GAPDH (Hs02758991_g1), T-cad (Hs01004530_m1), vWF (Hs01109446_m1), CD31 (Hs00169777_m1), KDR (Hs00911700_m1), CD105 (Hs00923996_m1), CD106 (Hs01003372_m1), CD146 (Hs00174838_m1), ALP (Hs01029144_m1), COL1 (Hs00164004_m1), Runx2 (Hs00231692_m1), OPN (Hs00959010_m1), OPG (Hs00171068_m1), OCN (Hs01587814_g1), CD90 (Hs00264235_s1), and ACTA2 (Hs00426835_g1) were all provided by Assays-on-Demand Gene Expression Products (Applied Biosystems).

In Vitro 3D Culture on Scaffolds in a Bioreactor

Hydroxyapatite scaffolds (Engipore, Finceramica-Faenza) in the form of porous cylinders (8 mm diameter, 4 mm height) were placed into chambers of a previously developed perfusion-based bioreactor system.[53] This device includes a perfusion chamber allocating the 3D porous scaffold that is perfused by culture media introduced inside the bioreactor. A pump connected to the bioreactor generates fluid flow in alternate directions directly through the scaffold allowing to generate defined flow velocities and homogeneous cell seeding through the scaffold. Cells (1 × 10^6) were suspended in 2 mL of CM supplemented with 10 nM dexamethasone (#D4902, Sigma), 0.1 mM ascorbic acid (#A1300000, Sigma), and FGF-2 (5 ng/ml), named DAF medium, and the scaffolds were perfused in alternate directions at a flow rate of 1 mL/minute through the scaffold pores for 1 week, as previously described.[37]

Quantification of Growth Factors in Bioreactor Supernatant

To determine the amount of growth factors in bioreactor supernatant before implantation, culture medium after the 1 week culture period was analyzed using VEGF ELISA kit (#DY293B, R&D Systems), IGF-1 ELISA kit (#DY291, R&D Systems), Adiponectin ELISA kit (#DY1065, R&D Systems), and Thrombospondin ELISA kit (#ab193716, Abcam). The

concentration of growth factors was normalized to the total amount of protein measured by the BCA quantification kit.

Assessment of In Vivo Bone Formation

In vivo, ectopic bone formation was assayed as previously described.[37] Briefly, after 1 week of 3D culture within a perfusion-based bioreactor, cellularized Engipore scaffolds were implanted in subcutaneous pouches created in the dorsum or the cervical region of 4-6-week-old CD1 nu/nu female nude mice (Charles River) for 12 weeks. Four constructs, based on 2 different human donors were implanted per mouse. Animals were treated in accordance with the Swiss Federal guidelines for animal welfare, after approval by the Veterinary Office of the Canton of Basel-Stadt (Cantonal permission BS1797). After 12 weeks, the constructs were harvested, fixed overnight in 4% formalin, completely decalcified with EDTA-based solution at 37°C, and paraffin-embedded. Sections (7 µm) were sliced along the length of the construct and stained with Masson's trichrome, observed microscopically to detect the formation of bone tissue for qualitative analysis, and then subjected to quantitative analysis of bone tissue by computerized bone histomorphometry as previously described.[52] Briefly, bright field images of sections at different depths of each construct were acquired and used to measure the area covered with bone tissue.

Assessment of In Vivo Vascularization

In vivo, ectopic vascularization was assayed as follows. After 1 week of 3D culture within the perfusion-based bioreactor, cellularized Engipore scaffolds were implanted subcutaneously in nude mice (Charles River). The scaffolds were harvested after 12 weeks, fixed overnight in 4% formalin, completely decalcified with EDTA-based solution at 37°C, and paraffin-embedded. Sections (7 µm) were sliced along the length of the scaffold. Epitope retrieval treatment was performed after rehydration, and samples were stained with CD31 antibody specific for human epitope at 1:250 (#ab32457, Abcam) or vWF antibody at 1:2000 (#M0616, Dako). Fluorescent-conjugated secondary antibodies chicken anti-rabbit Alexa 488 (#A-21441, Thermo Fischer Scientific) and goat anti-mouse Alexa 546 (#A-11030, Thermo Fischer Scientific) were used at 1:500. Stained sections were examined microscopically to quantify the blood vessels of human or mouse origins: fluorescent field images of sections of each construct were acquired and used to count CD31- or vWF-positive blood vessels.

In Situ Hybridization

To detect repetitive human-specific ALU sequences, chromogenic in situ hybridization was performed on paraffin sections of the in vivo constructs as described previously.[52] To improve the binding of the probe, one base of the sequence was changed from 59-cgaggcgggtggatcatgaggt-39, and reverse 59-ttttttgagacggagtctcgc-39 to respectively 59-cgaggcgggtgcatcatgaggt- 39, and reverse 59-ttttttgagacggagtctcgc-39.

Microtomography

Eight-week in vivo implants were fixed in formalin and stored in PBS. Micro-computed tomography (micro-CT) data were acquired from the implants using a phoenix nanotom m scanner (General Electric) with 0.5-mm aluminum filtered x-rays (applied voltage 70 kV; current 260 mA). Transmission images were acquired during a 360° scan rotation with an incremental rotation step size of 0.25°. Reconstruction was performed using a modified Feldkamp algorithm at an isotropic voxel size of 25 µm. Threshold-based segmentation and 3D measurement analyses (bone mineral density and volume) were performed using ImageJ software[54] with the BoneJ[55] and 3D Shape[56] extensions. For quantification of bone mineral density and volume, all data were normalized to the size of each construct. Three-dimensional rendering of the structures was performed using VGStudio MAX 2.2 software (Volume Graphics).

Lentiviral Transduction

T-cadherin was stably overexpressed in ASCs (ASCs (T-cad+)) and human umbilical vein ECs (HUVECs (T-cad+)) using pLVX-puro vector carrying full length human T-cad cDNA.[43] Cells transduced with an empty pLVX-puro vector served as controls. ASCs (at passage 2-3) and HUVECs (at passage 2) were transduced, puromycin-selected (1 µg/mL), and used up to passage 3-5. The expression of T-cad protein was monitored by immunoblotting.

Co-culture with HUVECs

Co-cultures contained a mixture (2:3) of HUVECs and either SVF cells, Unpass cells, or expanded ASCs (at P2-P3). The co-culture ratio (2:3) was determined according to the percentage of T-cad-positive cells measured in the SVF after flow cytometry analysis. Cells were maintained in osteogenic medium (CM supplemented with 10 nM dexamethasone (#D4902, Sigma), 0.1 mM ascorbic acid (#A1300000, Sigma) and 10 mM β-Glycerophosphate (#G9422, Sigma)) for 2D monolayer culture or in DAF medium for 3D scaffold culture in the perfused bioreactor system. In 2D, cells were seeded at a concentration of 1×10^4 cells/cm^2, and in the perfusion-based bioreactor, cells were seeded 1×10^6 cells within 2 mL of culture medium.

In Vitro Adipogenic, Osteogenic, and Chondrogenic Differentiation Assay

Before differentiation, cells were plated at 1×10^4/cm^2. Adipogenic, osteogenic, and chondrogenic lineage differentiation was performed by culture in specific media over 21 days. Adipogenic differentiation medium was composed of CM supplemented with 400 nM insulin (#I9278, Sigma), 100 nM dexamethasone (#D4902, Sigma), 50 µM indomethacin (#I7378, Sigma) and 500 µM IBMX (#I5879, Sigma). Osteogenic differentiation medium was composed of CM supplemented with 10 nM dexamethasone (#D4902, Sigma), 0.1 mM ascorbic acid (#A1300000, Sigma), and 10 mM β-Glycerophosphate (#G9422, Sigma). Chondrogenic differentiation medium consisted of CM without FBS supplemented with 0.1 mM ascorbic acid (#A1300000, Sigma), 100 nM dexamethasone (#D4902, Sigma), and 10 nM TGF-β3 (#243-B3/CF, R&D Systems): here cells were first cultured as pellets and then incubated as previously described.[57] Biochemical stainings with Alizarin red, Oil-red-O, and Safranin-O were used to respectively assess the osteogenic, adipogenic, and chondrogenic differentiation of the cells, as previously described.[58-60] The analysis of GAG content was studied as described previously.[52]

Statistical analysis

Results are expressed as mean ± SD. Before statistical testing, the Shapiro-Wilk test was performed on all data sets to assess

normal distribution. When data did not satisfy the normality test, they were analyzed with the nonparametric Kruskal-Wallis test for multiple comparisons and Dunn's post-hoc test or with Mann-Whitney test for single comparison. Data sets that passed the normality test were analyzed with 1-way ANOVA with Bonferroni's or Dunnet's post-test for multiple comparisons or with a *t*-test for a single comparison. Results were considered to be statistically significant at P values < .05 (*/P < .05, **/P < .01, ***/P < .001, and ****P < .0001). The data were processed with GraphPad Prism 5 Software (GraphPad, San Diego, CA).

Results

T-cadherin Is Expressed by the Endothelial Lineage Fraction of SVF, Unpass Cells, ASCs, and Native Adipose Tissue

Expression of T-cad protein was assessed by immunoblotting in freshly isolated SVF cells, in ASCs at different passages (from P0 to P4), and in ASCs cultured without passaging for 4 weeks (Unpass). The strong expression of both isoforms of T-cad (105 and 130 kDa) was initially evident in SVF cells and decreased with passaging, whereas expression in Unpass cells was maintained (Fig. 1A). Analysis of T-cad expression with normalization to the expression of internal loading control protein (β-actin at 42 kDa and GAPDH at 36 kDa), revealed that already at the first expansion (passage) on tissue culture plastic (P0), T-cad protein expression was significantly lower in ASCs than in freshly isolated SVF or Unpass cells (Fig. 1B). Immunofluorescence staining of T-cad in native human adipose tissue identified a specific subset of cells that expressed T-cad at the level of blood vessels and capillaries (Fig. 1C-E), co-localized with the endothelial markers vWF (Fig. 1C) and CD31 (Fig. 1E), and were in contact with the basement membrane marker Laminin (Fig. 1D). In Unpass cells, T-cad was expressed only in vascular-like structures containing ECs (Fig. 1F-H) and in endothelial tip-like cells (white circle). Moreover, concerning ASCs from P0 to P4, the proportion of cells expressing T-cad was extremely low, and no structure also positive for the endothelial marker was visible (data not shown). To establish that T-cad-positive cells in human adipose tissue are ECs, we sorted T-cad-positive cells from SVF and Unpass cells (Supplementary Fig. 1A and B, respectively) and analyzed the relative gene expression of endothelial and mesenchymal markers on the T-cad-depleted populations. SVF and Unpass cells depleted of T-cad-positive cells (Fig. 1I) exhibited a parallel, strong depletion of the endothelial markers vWF, CD31, and vascular endothelial growth factor receptor 2 (aka. KDR) (Fig. 1J-L), whereas expression of the mesenchymal markers CD105, CD73, and CD90 was unchanged (Fig. 1M-O). The evolution showing a higher percentage of ASC expressing the immunophenotypical subsets (CD105, CD73, and CD90) during expansion in vitro (data not shown) was in accordance with a recently published study.[61] These findings indicate that expression of T-cad is associated with ECs and is preserved under culture conditions enabling EC maintenance.

Bone Formation Potential by SVF and Unpass Cells Is Abolished After Depletion of T-cad-positive Cells

We have previously shown that SVF and Unpass cells can form ectopic bone tissue in vivo after 8 weeks if cultured within a ceramic scaffold for 5 days in a perfusion bioreactor system before implantation.[37] The specific contribution of T-cad-positive cells to osteogenicity of SVF and Unpass cells was investigated through depletion experiments (Fig. 2). SVF cells (Fig. 2A) and Unpass cells (Fig. 2C) reproducibly generated bone tissue in vivo (60 and 40% of all implants formed bone, respectively, Fig. 2E). In contrast, after depletion of T-cad-positive cells by FACS, neither SVF cells nor Unpass cells produced ectopic bone in vivo (Fig. 2B,D, and E), suggesting that the presence of the T-cad-positive cell population is crucial for bone formation by SVF and Unpass cells. Bone formation capacities under the different experimental conditions paralleled the amount of human, donor-derived blood vessels in the explanted osteogenic grafts (Fig. 2F), while the total blood vessel density (ie, both human and mouse blood vessels) remained constant (Fig. 2G). This suggests that the formation of a critical density of human blood vessels in the graft, and not the overall vascular density, is important to support bone formation by adipose tissue-derived stromal cells. As reported previously,[34] we found a direct contribution of human ALU-positive cells in bone formation by SVF cells (Fig. 2H,L, and P) and Unpass cells (Fig. 2J,N, and R), here indicated by black arrows. Under depletion conditions, human cells were also present in the fibrous tissue and at the border of blood vessels lumen (black arrows) formed after 8 weeks in vivo for the SVF (Fig. 2I,M, and Q), and Unpass condition (Fig. 2K,O, and S).

Depletion of T-cad-positive Cells from SVF and Unpass Cells Alters Secretion of Growth Factor and Expression of Endothelial and Bone Markers During 3D Bioreactor Culture

To identify possible mechanisms underlying the differential effect of the presence or absence of T-cad-positive cells on the in vivo osteogenic potential of SVF and Unpass cells, culture supernatants and cellular composition/phenotype were analyzed at the end of the in vitro bioreactor culture period (before implantation). In supernatants, only VEGF levels (Fig. 3A) followed the same trend as in vivo bone formation capacities, while this was not consistently the case for several other proteins known to regulate bone formation, including Adiponectin (Fig. 3B),[62] Thrombospondin (Fig. 3C),[63] IGF-1 (Fig. 3D),[64] BMP-4 (Fig. 3E), and BMP-2 (Fig. 3F). Amounts of Adiponectin and IGF-1 correlated with bone formation capacity of SVF but not that of Unpass cells, suggesting that some relevant cell population is lost during the transition from SVF to Unpass condition. At the cellular level, gene expression of vWF paralleled that of T-cad (Fig. 3G,H) and correlated with bone formation in vivo, thus indicating an endothelial-dependent contribution to the osteogenic potential of SVF and Unpass cells. Concerning the osteoblastic markers tested, gene expression of OPG, OPN, and Runx2 (Fig. 3K-M) but not ALP (Fig. 3I), or COL1 (Fig. 3J) correlated with T-cad gene expression.

Co-culture with HUVECs Rescues In Vivo Osteogenic and Vasculogenic Potential of T-cad-depleted SVF and Unpass Cells

To determine whether the pro-osteogenic role of the T-cad-positive cell population is directly linked to their endothelial nature, we performed rescue experiments using an exogenous source of ECs (HUVECs). The co-culture of HUVECs with T-cad-depleted SVF cells during in vitro bioreactor culture restored the capacity for bone formation in vivo (Fig. 4A-F). Human implanted cells again contributed to both bone and

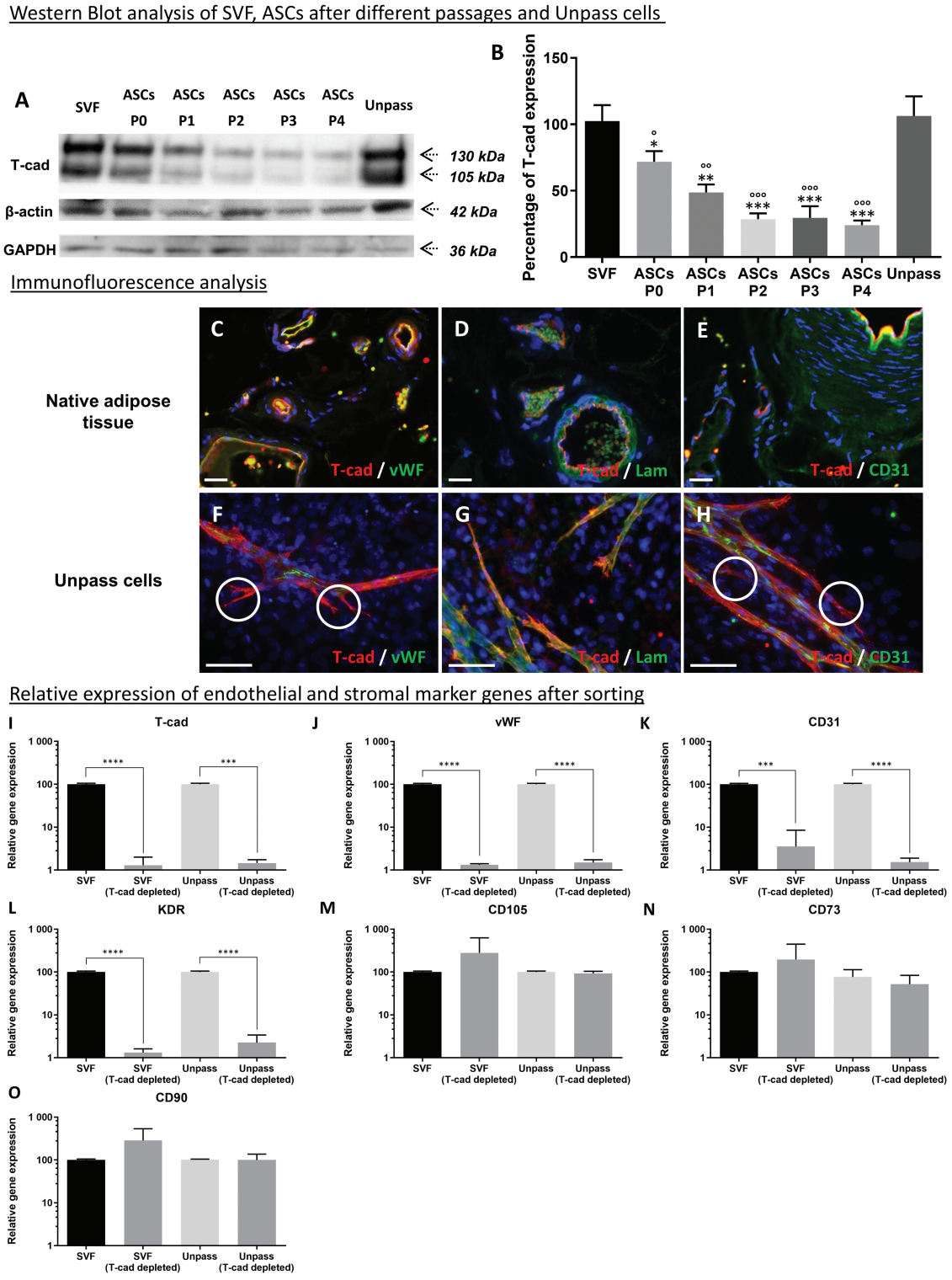

Figure 1. In vitro characterization and analysis of gene expression markers of the Tcadherin population in native human adipose tissue and Unpass cells. (**A**) Representative Western Blot of SVF, ASCs passed until passage 4 (P0, P1, P2, P3, and P4) and Unpass cells for T-cadherin, β-actin, and GAPDH. (**B**) Quantification of T-cad protein amount relative to β-actin and GAPDH protein amount (mean ± SD) in Western Blot assay. * shows the significant representation with the SVF condition and ° shows the significant representation with the Unpass condition. (**C-E**) Immunofluorescence on native human adipose tissue co-stained (C) for T-cad and vWF, (D) for T-cad and Laminin, and (E) for T-cad and CD31. (**F-G**) Immunofluorescence on Unpass cells co-stained (F) for T-cad and vWF, (G) for T-cad and Laminin, and (**H**) for T-cad and CD31. DAPI staining in blue shows the nuclei and the yellow/orange color indicates colocalization of T-cad with either vWF, Lam or CD31. (IO) Relative gene expression (mean±SD) of (**I**) T-cad, (**J**) vWF, (**K**) CD31, (**L**) KDR, (**M**) CD105, (**N**) CD73, and (**O**) CD90 of SVF, SVF depleted of T-cad cells, Unpass cells and Unpass cells depleted of T-cad cells. Scale bar in micrographs = 100 μm. $n = 7$ values per group for Western Blot quantification, and $n = 7$ values per group for qPCR analysis. Abbreviation: SVF, Stromal Vascular Fraction; ASCs, Adipose Stromal Cells; T-cad, T-cadherin; vWF, von Willebrand Factor; Lam, Laminin; KDR, kinase insert domain receptor. */°$P < .05$, **/°°$P < .01$, ***/°°°$P < .001$, ****$P < .0001$.

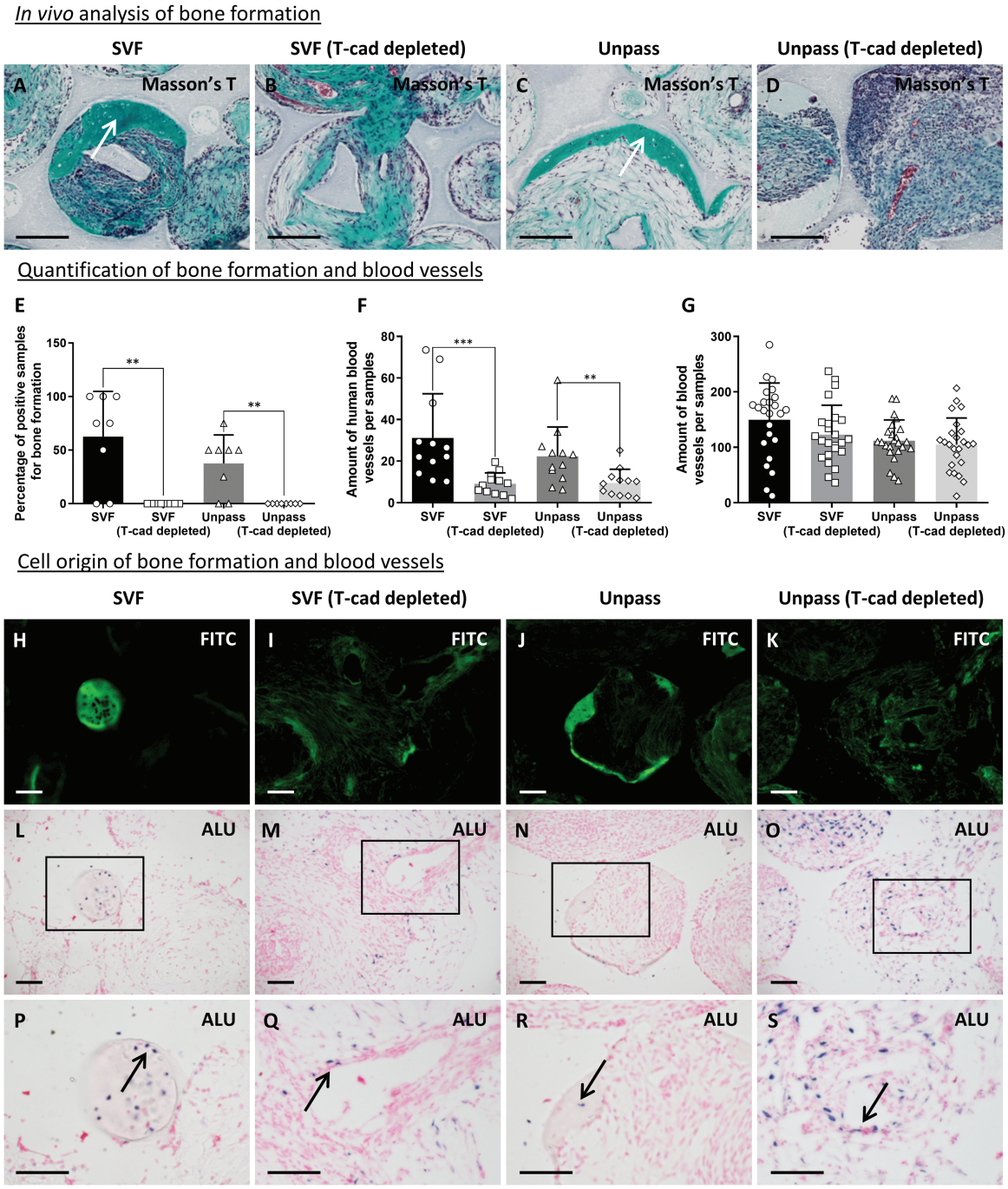

Figure 2. Depletion of T-cad-positive cells from SVF and Unpass cells impairs *in vivo* bone formation and vascularization. 12 weeks after *in vivo* implantation of Engipore samples seeded with SVF, SVF depleted of Tcad- positive cells, Unpass cells, and Unpass cells depleted of T-cad-positive cells were analysed for (**A-D**) Masson's Trichrome staining, (**E**) bone formation, (**F**) amount of the blood vessels of human origin (**G**) total amount of blood vessels, (**H-K**) autofluorescence in FITC channel, (**L-S**) human ALU staining. White arrows in (A) and (C) indicate bone tissue. Black arrows in (P-S) indicate ALU-positive cells. Scale bar in micrographs = 100 μm. Data in histograms are given as (mean ± SD). $n = 8$ values per group for bone formation quantification, $n = 24$ values per group for total blood vessel quantification, and $n = 12$ values per group for human blood vessel quantification. Abbreviation: Masson's T, Masson's Trichrome. $^{**}P < .01$, $^{***}P < .001$.

blood vessel formation (Fig. 4G-I). The rescue was almost total for bone formation (Fig. 4J), but only partial for blood vessel formation (Fig. 4K). Total blood vessel densities were comparable under the different conditions (Fig. 4L). The above in vivo findings were recapitulated in rescue experiments performed on depleted Unpass cells: co-culture of HUVECs with T-cad-depleted Unpass cells restored bone formation totally and vessel formation only partially, and did not impact total blood vessel density (Supplementary Figure 2). Taken together, these experiments demonstrate that human ECs are indispensable for bone formation in vivo by adipose tissue-derived stromal cells.

The analysis of supernatants collected at the end of in vitro culture in the perfusion bioreactor (Fig. 5) showed that the levels of VEGF (Fig. 5A) and Adiponectin (Fig. 5B) from HUVECs/T-cad-depleted SVF cells co-cultures was

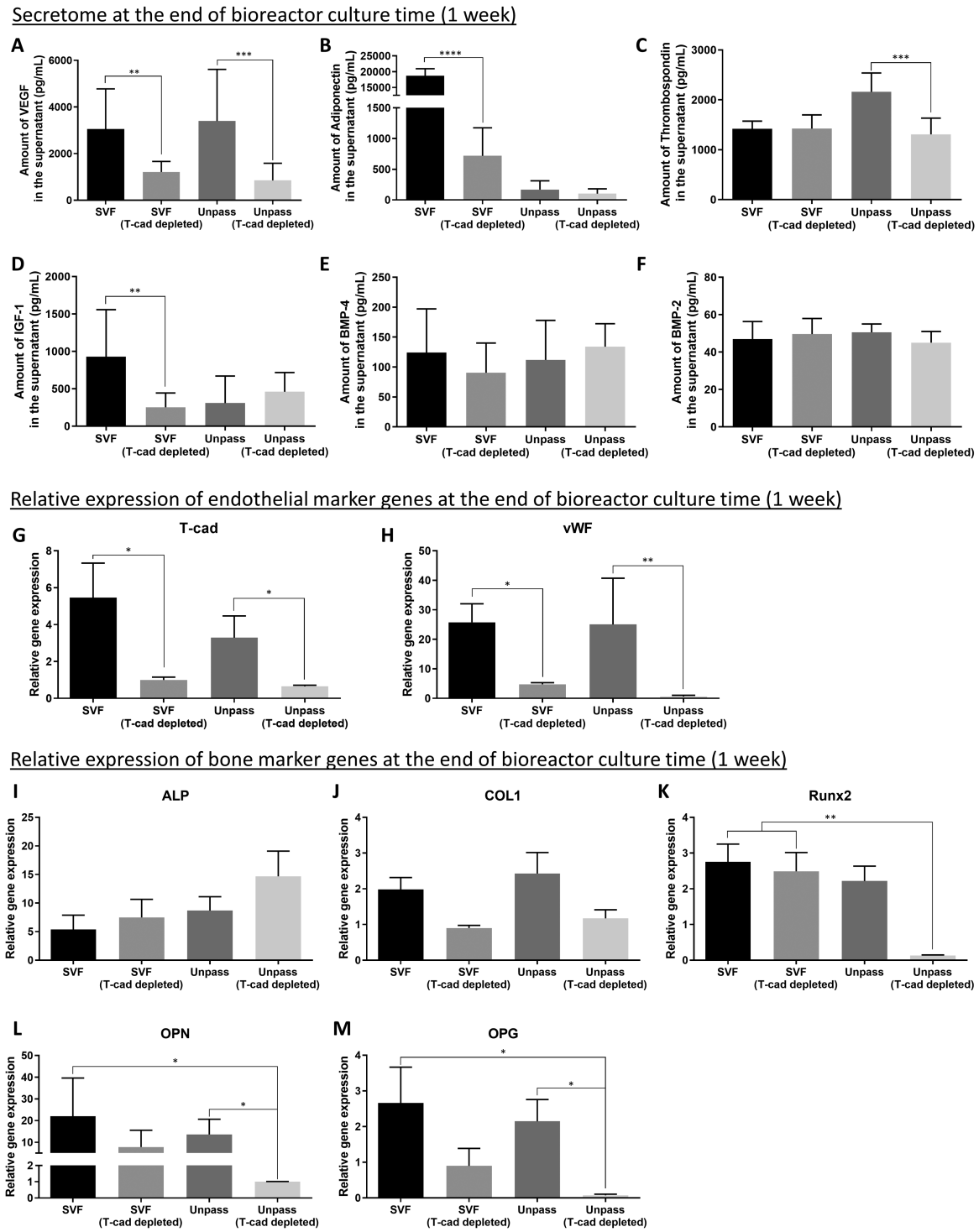

Figure 3. Depletion of T-cad-positive cells from SVF and Unpass cells alters secretion of growth factor and expression of endothelial and bone markers during 3D bioreactor culture. One week after pre-implantation bioreactor culture of Engipore samples seeded with SVF, SVF depleted of T-cad-positive cells, Unpass cells and Unpass cells depleted of T-cad-positive cells, perfusion supernatants were collected and analysed for release of growth factors (**A**) VEGF, (**B**) Adiponectin, (**C**) Thrombospondin, (**D**) IGF-1, (**E**) BMP-4 and (**F**) BMP-2, and resident cells analysed for relative gene expression of endothelial markers (**G**) T-cad and (**H**) vWF and bone markers (**I**) ALP, (**J**) Col1, (**K**) Runx2, (**L**) OPN, and (**M**) OPG. Data are given as (mean ± SD). $n = 12$ values per group for supernatant analysis, and $n = 6$ values per group for qPCR analysis. Abbreviations: VEGF, vascular endothelial growth factor; IGF, insulin-like growth factor; BMP, bone morphogenetic protein; T-cad, T-cadherin; vWF, von Willebrand factor; ALP, alkaline phosphatase; COL1, collagen type 1A1; Runx2, runt-related transcription factor 2; OPN, osteopontin; OPG, osteoprotegerin. $*P < .05$, $**P < .01$, $***P < .001$.

fully restored to that secreted by native SVF cells. Co-culture only partially restored levels of IGF-1 (Fig. 5C) to the native condition and was without effect on Thrombospondin (Fig. 5D). Co-culture of HUVECs with T-cad-depleted Unpass cells fully rescued secretion of VEGF and Thrombospondin and partially of Adiponectin during in vitro bioreactor culture (Supplementary Fig. 3). In the absence of a control with HUVECs only, however, we could not discriminate the specific contribution of HUVECs or SVF cells to this increased protein expression and only considered the total resulting

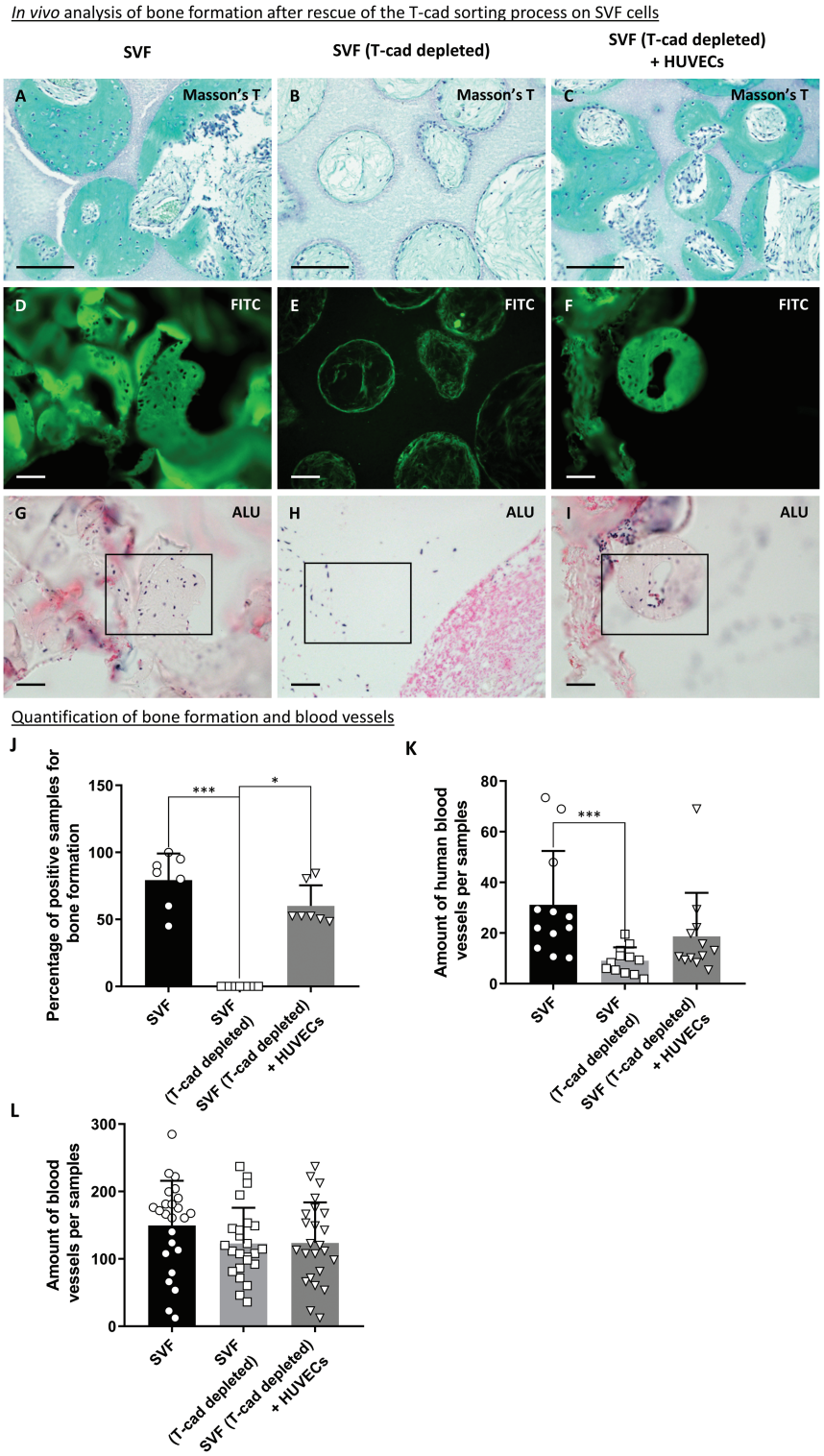

Figure 4. Impaired in vivo bone formation and vascularization capacities of T-cad-positive cell depleted SVF are rescued by co-culture with HUVECs. Twelve weeks after in vivo implantation, Engipore samples seeded with SVF, SVF depleted of Tcad-positive cells, and SVF depleted of T-cad-positive cells in co-culture with HUVECs were analysed for (**A-C**) Masson's Trichrome staining, (**D-F**) autofluorescence in FITC channel, (**G-I**) human ALU immunostaining, (**J**) bone formation, (**K**) amount of blood vessels of human origin, (**L**) total amount of blood vessels. Scale bar in micrographs = 100 μm. Data in histograms are given as (mean ± SD). $n = 7$ values per group for bone formation quantification, $n = 24$ values per group for total blood vessel quantification, and $n = 12$ values per group for human blood vessel quantification. Abbreviation: Masson's T, Masson's Trichrome. $*P < .05$, $***P < .001$.

expression level. Interestingly, and distinct from the SVF setting (Fig. 5C,D), depletion of Unpass cells did not impact IGF secretion and decreased thrombospondin secretion (Supplementary Fig. 3C,D). In both co-culture settings, the presence of HUVECs did not significantly increase T-cad gene expression levels (Fig. 5E and Supplementary Fig. 3E). Cellular vWF gene expression at the end of the bioreactor culture period was dramatically elevated in the HUVEC

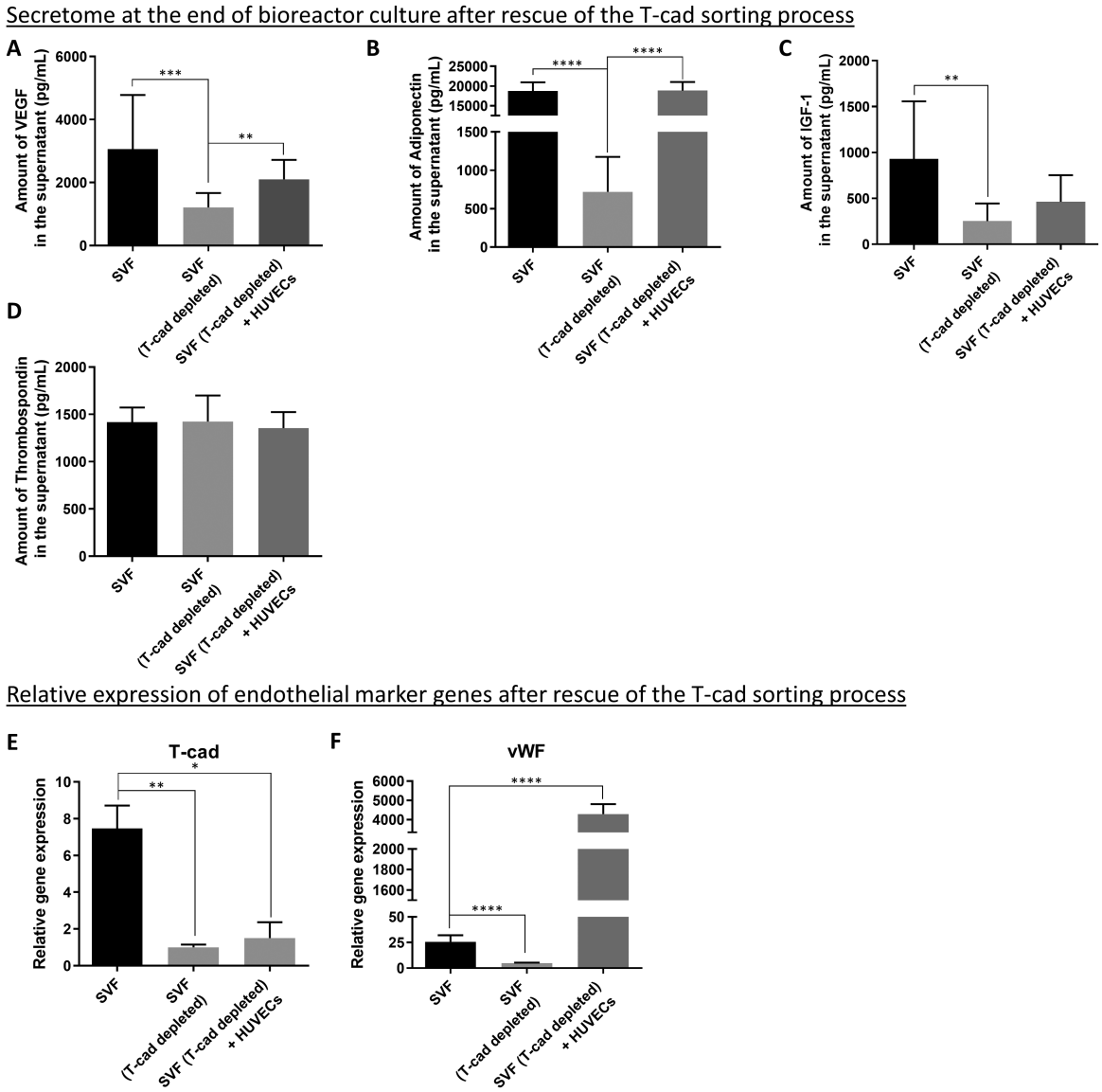

Figure 5. Co-culture of SVF depleted of T-cad-positive cells with HUVECs normalizes growth factor secretion and expression of endothelial and bone markers. One week after pre-implantation bioreactor culture of Engipore samples seeded with SVF, SVF depleted of T-cad-positive cells, and SVF depleted of T-cad-positive cells in co-culture with HUVECs, perfusion supernatants were collected and analysed for released growth factors (**A**) VEGF, (**B**) Adiponectin, (**C**) IGF-1, and (**D**), Thrombospondin, and resident cells were analysed for relative gene expression of endothelial markers (**E**) T-cad, and (**F**) vWF. Data in histograms are given as (mean ± SD). $n = 12$ values per group for supernatant analysis, and $n = 6$ values per group for qPCR analysis. Abbreviations: VEGF, vascular endothelial growth factor; IGF, insulin-like growth factor; BMP, bone morphogenetic protein; T-cad, T-cadherin; vWF, von Willebrand factor. $*P < .05$, $**P < .01$, $***P < .001$, $****P < .0001$.

co-culture settings, achieving levels approximately 200- and 70-fold greater than that in the native SVF and Unpass cells, respectively (Fig. 5F and Supplementary Fig. 3F). These data suggest that ECs and endothelial-derived angiogenic modulators contribute to the potentiation of angiogenesis by adipose tissue-derived stromal cells.

Upregulation of T-cad on Co-cultured HUVECs Positively Affects Osteogenic and Vasculogenic Potential of T-cad-depleted SVFs and Unpass Cells In Vivo

To investigate the role of T-cad expression on ECs and the potential interaction between T-cad-positive cells and stromal cells from adipose tissue, we overexpressed T-cad in HUVECs (HUVECs T-cad+) by lentiviral transduction (Supplementary Fig. 4). T-cad gene expression in HUVECs (T-cad+) was increased by 60-fold as compared control HUVECs (Supplementary Fig. 4A). Control HUVECs and HUVECs (T-cad+) exhibited the same relative gene expression profile for the endothelial markers vWF (Supplementary Fig. 4B), KDR (Supplementary Fig. 4C), and CD105 (Supplementary Fig. 4D), but did not express the mesenchymal marker CD90 (Supplementary Fig. 4E).

To investigate whether T-cad protein expression or the endothelial identity of cells present in the human adipose tissue population is critical for bone formation in vivo, we performed rescue experiments through co-culture of HUVECs (T-cad+) or control HUVECs with T-cad-depleted SVF and Unpass cells (Fig. 6). As depicted in the photomicrographs (Fig. 6A-D), in vivo bone formation capacities of SVF cells or Unpass cells that had been depleted of T-cad-positive cells were restored by co-culture with HUVECs

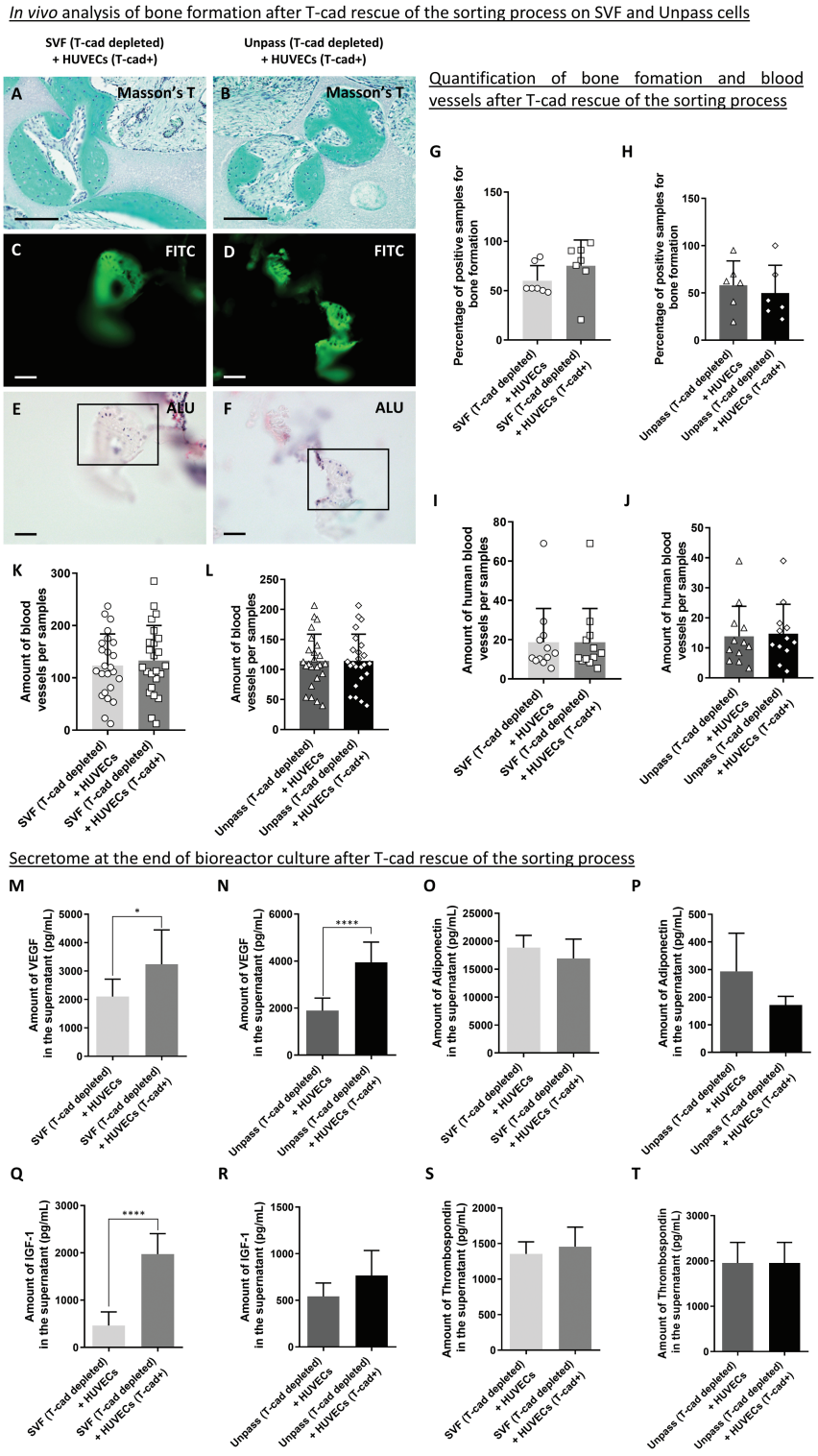

Figure 6. In vivo assessment and quantification of bone formation and vascularization after the rescue of T-cad depletion in SVF and Unpass cells by co-culture with control HUVECs or HUVECs overexpressing T-cad. Twelve weeks after in vivo implantation, Engipore samples were seeded with (**A, C, E, G, I, K, M, O, Q**, and **S**) SVF depleted of T-cad-positive cells in co-culture with control HUVECs or HUVECs (T-cad+) and (**B, D, F, H, L, N, P, R**, and **T**) Unpass cells depleted of T-cad-positive cells in co-culture with control HUVECs or HUVECs (T-cad+). (A, B) Masson's Trichrome staining, (C, D) autofluorescence in FITC, (E, F) human ALU immunostaining, (G, H) bone formation, (I, J) amount of blood vessels of human origin and (K, L) total amount of blood vessels were analysed. (M-T) Perfusion supernatants collected after 1 week of pre-implantation bioreactor culture of Engipore samples seeded with (M, O, Q, T) SVF depleted of T-cad-positive cells in co-culture with control HUVECs or HUVECs (T-cad+) and (N, P, R, and T) Unpass cells depleted of T-cad-positive cells in co-culture with control HUVECs or HUVECs (T-cad+). Secreted growth factors (M, N) VEGF, (O, P) Adiponectin, (Q, R) IGF-1 and (S, T) Thrombospondin were analysed. Scale bar in micrographs = 100 μm. Data in histograms are given as (mean ± SD). $n = 7$ values per group for bone formation quantification, $n = 24$ values per group for total blood vessel quantification, $n = 12$ values per group for human blood vessel quantification, and $n = 12$ values per group for supernatant analysis. $*P < .05$, $****P < .0001$.

(T-cad+). Moreover, as revealed by ALU staining, human implanted cells again contributed to bone formation (Fig. 6E,F). HUVECs (T-cad+) and control HUVECs comparably rescued the in vivo osteogenic (Fig. 6G,H) and vasculogenic (Fig. 6K,L) capacities of the depleted SVF and Unpass cells, while not affecting the total blood vessel density (Fig. 6I,J). Analysis of supernatants following bioreactor co-culture indicated that control and T-cad-overexpressing HUVECs could differently affect secretome content (Fig. 6M-T). VEGF secretion was significantly greater for SVF and Unpass cells co-cultured with HUVECs (T-cad+) (vs control HUVECs, Fig. 6M,N). IGF-1 secretion was significantly greater for SVF (but not Unpass cells) co-cultured with HUVECs (T-cad+) (vs control HUVECs, Fig. 6Q,R). HUVECs (T-cad+) and control HUVECs comparably affected the secretion of Adiponectin (Fig. 6O,P) and Thrombospondin (Fig. 6S,T). Cellular gene expression analysis at the end of the bioreactor culture period (Fig. 7) confirmed the overexpression of T-cad (Fig. 7A,B) in co-cultures containing HUVECs (T-cad+). Moreover, vWF gene expression in the co-cultures was not affected by the level of T-cad expression on HUVECs (Fig. 7C,D). Gene expression levels of the osteoblastic markers ALP, COL1, Runx2, OPG, and OPN were higher in co-cultures containing HUVECs (T-cad+) (Fig. 7E-N). Overall, these data demonstrate that while the elevation of T-cad expression on ECs might impact osteogenic outcome through enhancing osteoblastic gene expression in stromal cells, it is the presence of an EC population per se in adipose tissue-derived stromal/stem cells that is essential for in vivo bone formation.

Co-culture of Expanded ASCs with T-cad Overexpressing HUVECs in 2D Monolayer Positively Affects Angiogenic and Osteogenic Profiles

We examined the effect of co-culturing expanded ASCs (at P2-P3) with control HUVECs or HUVECs (T-cad+) on angiogenic behavior, bone marker gene expression, and mineralization in vitro (Supplementary Fig. 5). Compared with monoculture ASCs and the ASCs/control HUVECs co-culture, T-cad gene expression in the ASCs/HUVECs (T-cad+) co-culture remained fully elevated during the first week of culture in osteogenic medium and thereafter declined (Supplementary Fig. 5A). The vWF gene expression in the ASCs/HUVECs (T-cad+) and ASCs/control HUVECs co-cultures during the first 2 weeks of culture was similarly elevated compared to ASCs monoculture, and thereafter decreased to parallel the low level of T-cad expression (Supplementary Fig. 5B). The angiogenic behavior of the cultures was assessed after 3 weeks by CD31 immunolabeling. Whereas monoculture ASCs were negative for CD31, co-cultures exhibited "islands"/areas of CD31-positive cells, with this being more prominent in the ASCs/HUVECs (T-cad+) co-culture (Supplementary Fig. 5C). Gene expression levels of early, mid, or late bone markers did not differ between co-culture and monoculture conditions at any of the time points examined (Supplementary Fig. 5D-H). Mineralization during osteogenic differentiation of the cultures was examined by Alizarin red staining. Visually, it was apparent that the onset of mineralization occurred earliest (within 1 week) in the ASCs/HUVECs (T-cad+) co-culture condition (Supplementary Fig. 5I). Solubilization and quantification of the stain confirmed a more rapid and extensive mineralization in the ASCs/HUVECs (T-cad+) co-culture than in the ASCs monoculture and ASCs/control HUVECs co-culture conditions (Supplementary Fig. 5J). These data suggest that ECs support the development of a pseudo-angiogenic network during osteogenic differentiation of ASCs.

3D Scaffold Co-culture of HUVECs and Expanded ASCs

We next queried whether the osteogenic potential of expanded ASCs (at P2-P3) might be rescued if co-cultured for 1 week in the 3D scaffold perfusion setting with control or T-cad overexpressing HUVECs. As expected, the T-cad gene was expressed in both co-culture sets with the greatest relative expression for ASCs/HUVECs (T-cad+) (Supplementary Fig. 6A). Gene expression of endothelial marker vWF was significantly higher in both co-culture sets as compared to monoculture ASCs (Supplementary Fig. 6B). Concerning the expression of genes for the early osteoblastic markers, only COL1 (Supplementary Fig. 6D) was significantly increased in 3D ASCs/HUVECs (T-cad+) and in ASCs/control HUVECs co-cultures as compared to mono-culture of ASCs. However, for other bone markers like ALP (Supplementary Fig. 6C), Runx2 (Supplementary Fig. 6E), and the late marker OPN (Supplementary Fig. 6G), or OCN (Supplementary Fig. 6F), no significant differences were observed. Overall, this suggests that ECs expressing high levels of T-cad can directly stimulate the collagen type 1 gene expression of expanded ASCs.[30,65]

T-cad Overexpression in Expanded ASCs Increases Mineralization But Does Not Affect Adipogenic and Chondrogenic Differentiation Capacity

To assess whether ASC differentiation capacity is affected by the expression of T-cad, we induced it in ASCs (at P2-P3) by lentiviral transduction, with untransfected ASCs and mock-transfected ASCs serving as controls (Supplementary Fig. 7). T-cad protein and gene expression in ASCs (T-cad+) was confirmed by Western blot and RT-PCR (Supplementary Fig. 7A,B). ASCs, ASCs (Mock), and ASCs (T-cad+) showed similar differentiation potential into adipocytes and chondrocytes (Supplementary Fig. 7C-E). For osteoblastic differentiation, ASCs (T-cad+) showed an increased mineralization potential as compared to controls (Supplementary Fig. 7E,F). Nevertheless, this stimulation of osteoblastic mineralization was not sufficient to make ASCs (T-cad+) frankly osteogenic in vivo (Supplementary Fig. 7H-J).

Discussion

Here, we discovered firstly that the stromal, osteoprogenitor component of SVF cells requires T-cad expressing ECs to be osteogenic, and secondly that these T-cad expressing cells can be found within the SVF or can be functionally substituted by exogenous HUVECs. We established that T-cad-positive cells in human adipose define a population of ECs which are differentially preserved depending on the in vitro culture conditions. The compromised in vivo bone formation capacity of ASCs at P0 and P4,[37] corresponds to culture conditions in which the T-cad-positive cell population is strongly reduced as compared to more osteogenic SVF and Unpass cells. Evidence for the pro-osteogenic role of those T-cad-positive cells was obtained through rescue experimentation, whereby the addition of HUVECs to SVF or Unpass cells previously depleted of T-cad-positive cells fully restored in vivo bone formation.

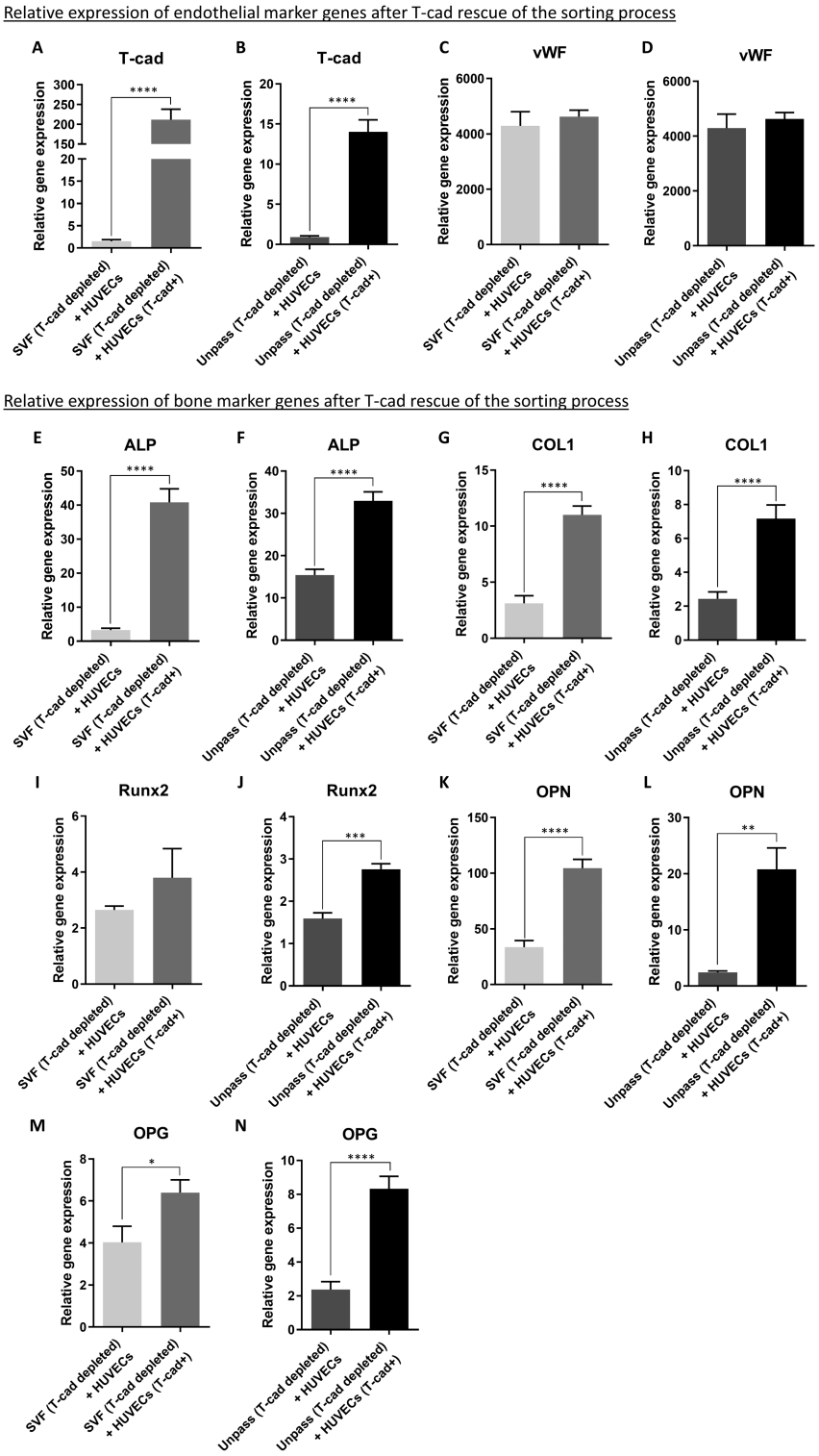

Figure 7. In vitro quantification of endothelial and bone markers relative gene expression after the rescue of T-cad depletion in SVF and Unpass cells by co-culture with control HUVECs or HUVECs overexpressing T-cad. Relative gene expression (mean ± SD) of endothelial markers (**A-B**) T-cad and (**C-D**) vWF and of bone markers (**E-F**) ALP, (**G-H**) COL1, (**I-J**) Runx2, (**K-L**) OPN, and (**M-N**) OPG in 2D cultures of SVF or Unpass cells depleted of T-cad-positive cells in co-culture with control HUVECs or with HUVECs (T-cad+). (E-N) $n = 6$ values per group for qPCR analysis. Abbreviations: T-cad, T-cadherin; vWF, von Willebrand factor; ALP, alkaline phosphatase; COL1, collagen type 1A1; Runx2, runt-related transcription factor 2; OPN, osteopontin; OPG, osteoprotegerin. $*P < .05$, $**P < .01$, $***P < .001$, $****P < .0001$.

Although research on signaling pathways has provided information on the effect of signaling molecules on cell migration, adhesion, proliferation, differentiation, and ultimately bone formation by ASCs, the mechanisms driving ASCs into the osteoblastic lineage are still not fully understood. Multiple signaling pathways were shown to participate in the differentiation from an osteoblastic progenitor to a committed osteoblast including transforming growth factor-β (TGF-β)/

bone morphogenetic proteins (BMPs), Wnt/β-Catenin, Notch, Hedgehog, and FGF.[66-68] Here, we observed the upregulation of 3 factors, IGF-1, Adiponectin, and VEGF, associated with induced bone formation capacity of ASCs. This is consistent with observations that VEGF stimulates the formation of a newly formed network of human blood capillaries, essential during the physiological process of bone regeneration.[69] IGF-1 has been shown to synergistically promote, together with erythropoietin, the osteoblastic differentiation of rat ASCs.[70,71] Concerning Adiponectin upregulation, it is well described in the literature that Adiponectin secreted from ASCs could directly inhibit adipogenesis in ASCs and BMSCs and promote osteogenesis.[62,71] This is concordant with previous reports on osteodifferentiated ASCs. For example, ASCs cultured with osteogenic medium produce pro-angiogenic factors responsible for vessel recruitment and angiogenesis.[31] Similarly, pre-osteodifferentiated ASCs can promote human microvascular EC recruitment and migration and enhance their functionality by inducing their ability to form capillary-like structures in vitro and in vivo, thus providing potential benefits in the clinical outcome (ie, promotion of angiogenesis/vascularization and bone formation).[31]

Strong crosstalk between osteoprogenitors and a functional vascular network triggers the processes of bone formation, remodeling, and healing. For this reason, EC recruitment and vascular organization are key in all these processes.[72-74] Therefore, osteoprogenitor/EC interactions should be promoted in vitro to recapitulate physiological conditions. There is much evidence of advantages conveyed through the use of co-cultures of ASCs with other cell types for the treatment of bone defects. For instance, ceramic scaffolds containing co-cultures of ASCs and BMSCs have proven more effective for the treatment of calvarial defects in mice as compared to ceramic with ASCs alone.[75] Another study on 3D-culture systems showed that the co-culture of ASCs with HUVECs increases the production of angiogenesis-related genes in both cell types and that these effects are mediated by the activation of the Wnt/β-catenin pathway.[76] A better understanding of cell-cell communication in adipose-derived cells is an important step toward developing tissue-engineering strategies that support both bone growth and vascular formation. The data obtained in this study suggest that enhanced vascularization is achieved through synergistic effects between the 2 cell compartments (stromal and endothelial), likely by the production of osteoblast-derived angiogenic factors. Osteogenic differentiation of ASCs is in turn increased by ECs, as previously described,[77,78] likely involving VEGF signaling.[79] Our study consistently found that the expression level of osteoinductive/osteogenic markers (ALP, COL1, OPN, and OPG) was lowered in SVF or Unpass cells following the depletion of their T-cad-positive cell population and restored to native levels by co-culture with HUVECs. Overexpression of T-cad in co-cultured HUVECs did not enhance bone formation in vivo despite the slightly stronger osteogenic commitment observed in vitro. Our findings contrast with in vivo findings by Seebach et al.[80] and by Sahar et al.,[81] who used ceramic scaffolds seeded with endothelial progenitor cells and osteodifferentiated ASCs and demonstrated less bone repair in the presence of ECs. However, our observations are consistent with several other reports demonstrating improved in vitro vascularization and in vivo bone formation[27,31,80,82] when ECs and osteoblasts are co-cultured. EC and osteoblast co-culture models have demonstrated cell-cell contact-dependent changes in gene expression patterns in both cell types. Those changes include up-regulation of VEGF receptor 2 in ECs and up-regulation of alkaline phosphatase in osteoblasts.[83,84] It is also clear that ECs improve human bone marrow stromal cell differentiation through direct cellular contact.[85] The precise mechanisms whereby ECs and/or progenitor ECs increase osteogenesis by adipose tissue-derived stromal/stem cells remain to be delineated.

We also observed that passaged ASCs overexpressing T-cad presented a higher mineralization level as compared to parental or mock-transfected ASCs, by as yet unknown mechanisms. On the other hand, T-cad overexpression in ASCs was without effects on adipogenic and chondrogenic differentiation. Chondrogenic differentiation was minimal in every experimental condition tested, which is concordant with the observation that ASCs secrete angiogenic factors which are detrimental to the differentiation of chondrocytes and can prevent cartilage regeneration.[86] Regarding the adipogenic differentiation, pre-adipocytes directly derive from the ASCs present in adipose tissue, and their generation may be inhibited by obesity-associated responses such as Adiponectin,[87] which we found to be overexpressed in the presence of ECs. Upregulation of Adiponectin in the HUVEC containing co-cultures is in agreement with findings that ECs are the source of paracrine factors that influence a pre-adipocyte generation and are required for the formation of new blood vessels that control blood supply to adipose tissue.[88] Moreover, endothelial progenitor cells are closely related to ASCs, as they are derived from them[89] or from circulating bone marrow-derived cells.[90] In conclusion, there is likely also a strong crosstalk between endothelial progenitors and ASCs controlling the homeostasis of adipose tissue formation, analogous to our observation herein for ECs and ASCs in bone tissue formation.

Our study supports that the presence of ECs exerts a major functional impact on osteogenic graft development. However, even though co-culture of ASCs with HUVECs almost completely rescued the bone-forming capacity of SVF and Unpass cells depleted of T-cad-positive cells, we cannot totally exclude a contribution by other cells in the SVF population. In this regard, analyzing other endothelial markers (eg, CD31, VE-cadherin, or vWF) present in the SVF population was challenging due to potential cross expression of endothelial markers in other cell populations such as monocytes or pre-adipocytes as already well described in the literature.[91-93]

The present study not only provides novel knowledge about the role of T-cad-positive (endothelial) cells residing in adipose tissue on the functionality of ASCs toward different mesenchymal lineages but could also find a practical application in tissue engineering approaches for bone regeneration and repair. The maintenance and the quantification of the T-cad-positive subpopulation of SVF or Unpassaged ASCs may be developed as a quality control to predict the potency of engineered osteogenic grafts based on adipose tissue cells. Alternatively, supplementation of expanded ASCs with ECs could be pursued as a strategy to restore and/or increase both the angiogenic and osteogenic potentials of the engineered constructs.

Conclusions

Here, we demonstrated that a subpopulation of SVF cells, namely T-cad-positive endothelial lineage cells supports angiogenic and osteogenic differentiation of adipose

tissue-derived cells. The endothelial nature of the T-cad-positive cells is the key feature to explain this effect, rather than the expression level of T-cad marker on those cells. Further studies in this field will be necessary to shed more light on the precise mechanisms involved in this crosstalk between ASCs and ECs.

Funding

This study was supported by the Swiss National Science Foundation, SNF grant # 310030-156291 (to A.S. and I.M.) and the Swiss Heart Foundation, grant FF18094 (to M.P.).

Conflict of Interest

The authors indicated no potential conflicts of interest.

Author Contributions

J.G.: study conception and design, acquisition of data, analysis and interpretation of data, writing of manuscript. B.D., A.F., S.P., T.I.: acquisition of data. D.J.S.: analysis and interpretation of data. M.P.: analysis and interpretation of data, writing of manuscript. T.J.R., I.M., A.S.: study conception and design, analysis and interpretation of data, writing of manuscript, financial support.

Data Availability

The data underlying this article will be shared on reasonable request to the corresponding author.

Supplementary Material

Supplementary material is available at *Stem Cells Translational Medicine* online.

References

1. Barabaschi GD, Manoharan V, Li Q, Bertassoni LE. Engineering pre-vascularized scaffolds for bone regeneration. *Adv Exp Med Biol*. 2015;881:79-94.
2. Rouwkema J, Rivron NC, van Blitterswijk CA. Vascularization in tissue engineering. *Trends Biotechnol*. 2008;26(8):434-441.
3. Novosel EC, Kleinhans C, Kluger PJ. Vascularization is the key challenge in tissue engineering. *Adv Drug Deliv Rev*. 2011;63(4-5):300-311.
4. Moon JJ, West JL. Vascularization of engineered tissues: approaches to promote angio-genesis in biomaterials. *Curr Top Med Chem*. 2008;8(4):300-310.
5. Miranville A, Heeschen C, Sengenès C, Curat CA, Busse R, Bouloumié A. Improvement of postnatal neovascularization by human adipose tissue-derived stem cells. *Circulation*. 2004;110(3):349-355.
6. Scherberich A, Galli R, Jaquiery C, Farhadi J, Martin I. Three-dimensional perfusion culture of human adipose tissue-derived endothelial and osteoblastic progenitors generates osteogenic constructs with intrinsic vascularization capacity. *Stem Cells*. 2007;25(7):1823-1829.
7. Mehrkens A, Saxer F, Güven S, et al. Intraoperative engineering of osteogenic grafts combining freshly harvested, human adipose-derived cells and physiological doses of bone morphogenetic protein-2. *Eur Cell Mater*. 2012;24:308-319.
8. Lattanzi W, Pola E, Pecorini G, Logroscino CA, Robbins PD. Gene therapy for *in vivo* bone formation: recent advances. *Eur Rev Med Pharmacol Sci*. 2005;9(3):167-174.
9. Lindroos B, Suuronen R, Miettinen S. The potential of adipose stem cells in regenerative medicine. *Stem Cell Rev Rep*. 2011;7(2):269-291.
10. Barba M, Cicione C, Bernardini C, Michetti F, Lattanzi W. Adipose-derived mesenchymal cells for bone regereneration: state of the art. *Biomed Res Int*. 2013;2013:416391.
11. Brennan MA, Renaud A, Guilloton F, et al. Inferior *in vivo* osteogenesis and superior angiogenesis of human adipose-derived stem cells compared with bone marrow-derived stem cells cultured in Xeno-free conditions. *Stem Cells Transl Med*. 2017;6(12):2160-2172.
12. Osinga R, Di Maggio N, Todorov A, et al. Generation of a bone organ by human adipose-derived stromal cells through endochondral ossification. *Stem Cells Transl Med*. 2016;5(8):1090-1097.
13. Dufrane D, Docquier PL, Delloye C, Poirel HA, André W, Aouassar N. Scaffold-free three-dimensional graft from autologous adipose-derived stem cells for large bone defect reconstruction: clinical proof of concept. *Medicine (Baltimore)*. 2015;94(50):e2220.
14. Shah FS, Li J, Dietrich M, et al. Comparison of stromal/stem cells isolated from human omental and subcutaneous adipose depots: differentiation and immunophenotypic characterization. *Cells Tissues Organs*. 2014;200(3-4):204-211.
15. Wen C, Yan H, Fu S, Qian Y, Wang D, Wang C. Allogeneic adipose-derived stem cells regenerate bone in a critical-sized ulna segmental defect. *Exp Biol Med (Maywood.)* 2016;241(13):1401-1409.
16. He J, Duan H, Xiong Y, et al. Participation of CD34-enriched mouse adipose cells in hair morphogenesis. *Mol Med Rep*. 2013;7(4):1111-1116.
17. De Francesco F, Tirino V, Desiderio V, et al. Human CD34/CD90 ASCs are capable of growing as sphere clusters, producing high levels of VEGF and forming capillaries. *PLoS One*. 2009;4(8):e6537.
18. Kapur SK, Katz AJ. Review of the adipose derived stem cell secretome. *Biochimie*. 2013;95(12):2222-2228.
19. Kilroy GE, Foster SJ, Wu X, et al. Cytokine profile of human adipose-derived stem cells: expression of angiogenic, hematopoietic, and pro-inflammatory factors. *J Cell Physiol*. 2007;212(3):702-709.
20. Ducy P. The role of osteocalcin in the endocrine cross-talk between bone remodelling and energy metabolism. *Diabetologia*. 2011;54(6):1291-1297.
21. Gómez-Ambrosi J, Rodríguez A, Catalán V, Frühbeck G. The bone-adipose axis in obesity and weight loss. *Obes Surg*. 2008;18(9):1134-1143.
22. Reid IR. Relationships between fat and bone. *Osteoporos Int*. 2008;19(5):595-606.
23. Dashnyam K, Buitrago JO, Bold T, et al. Angiogenesis-promoted bone repair with silicate-shelled hydrogel fiber scaffolds. *Biomater Sci*. 2019;7(12):5221-5231.
24. Rumney RMH, Lanham SA, Kanczler JM, et al. *In vivo* delivery of VEGF RNA and protein to increase osteogenesis and intraosseous angiogenesis. *Sci Rep*. 2019;9(1):17745.
25. He J, Han X, Wang S, et al. Cell sheets of co-cultured BMP-2-modified bone marrow stromal cells and endothelial progenitor cells accelerate bone regeneration *in vitro*. *Exp Ther Med*. 2019;18(5):3333-3340.
26. Grellier M, Bordenave L, Amédée J. Cell-to-cell communication between osteogenic and endothelial lineages: implications for tissue engineering. *Trends Biotechnol*. 2009;27(10):562-571.
27. Guerrero J, Oliveira H, Catros S, et al. The use of total human bone marrow fraction in a direct three-dimensional expansion approach for bone tissue engineering applications: focus on angiogenesis and osteogenesis. *Tissue Eng Part A*. 2015;21(5-6):861-874.
28. Guerrero J, Catros S, Derkaoui SM, et al. Cell interactions between human progenitor-derived endothelial cells and human mesenchymal stem cells in a three-dimensional macroporous polysaccharide-based scaffold promote osteogenesis. *Acta Biomater*. 2013;9(9):8200-8213.
29. Tamari T, Kawar-Jaraisy R, Doppelt O, Giladi B, Sabbah N, Zigdon-Giladi H. The paracrine role of endothelial cells in bone formation via CXCR4/SDF-1 pathway. *Cells*. 2020;9(6):1325.

30. Kocherova I, Bryja A, Mozdziak P, et al. Human umbilical vein endothelial cells (HUVECs) co-culture with osteogenic cells: from molecular communication to engineering prevascularised bone grafts. *J Clin Med*. 2019;8(10):1602.
31. Genova T, Petrillo S, Zicola E, et al. The crosstalk between osteodifferentiating stem cells and endothelial cells promotes angiogenesis and bone formation. *Front Physiol*. 2019;10:1291.
32. Farre-Guasch E, Bravenboer N, Helder MN, Schulten E, Ten Bruggenkate CM, Klein-Nulend J. Blood vessel formation and bone regeneration potential of the stromal vascular fraction seeded on a calcium phosphate scaffold in the human maxillary sinus floor elevation model. *Materials (Basel)*. 2018;11(1):161.
33. James AW, Zara JN, Corselli M, et al. An abundant perivascular source of stem cells for bone tissue engineering. *Stem Cells Transl Med*. 2012;1(9):673-684.
34. Güven S, Mehrkens A, Saxer F, et al. Engineering of large osteogenic grafts with rapid engraftment capacity using mesenchymal and endothelial progenitors from human adipose tissue. *Biomaterials*. 2011;32(25):5801-5809.
35. Najman SJ, Cvetković VJ, Najdanović JG, et al. Ectopic osteogenic capacity of freshly isolated adipose-derived stromal vascular fraction cells supported with platelet-rich plasma: A simulation of intraoperative procedure. *J Craniomaxillofac Surg*. 2016;44(10):1750-1760.
36. Rhee SC, Ji YH, Gharibjanian NA, Dhong ES, Park SH, Yoon ES. *In vivo* evaluation of mixtures of uncultured freshly isolated adipose-derived stem cells and demineralized bone matrix for bone regeneration in a rat critically sized calvarial defect model. *Stem Cells Dev*. 2011;20(2):233-242.
37. Di Maggio N, Martella E, Frismantiene A, et al. Extracellular matrix and α5β1 integrin signaling control the maintenance of bone formation capacity by human adipose-derived stromal cells. *Sci Rep*. 2017;7:44398.
38. Castro CH, Shin CS, Stains JP, et al. Targeted expression of a dominant-negative N-cadherin *in vivo* delays peak bone mass and increases adipogenesis. *J Cell Sci*. 2004;117(Pt 13):2853-2864.
39. Okazaki M, Takeshita S, Kawai S, et al. Molecular cloning and characterization of OB-cadherin, a new member of cadherin family expressed in osteoblasts. *J Biol Chem*. 1994;269(16):12092-12098.
40. Shin CS, Lecanda F, Sheikh S, Weitzmann L, Cheng SL, Civitelli R. Relative abundance of different cadherins defines differentiation of mesenchymal precursors into osteogenic, myogenic, or adipogenic pathways. *J Cell Biochem*. 2000;78(4):566-577.
41. Kawaguchi J, Kii I, Sugiyama Y, Takeshita S, Kudo A. The transition of cadherin expression in osteoblast differentiation from mesenchymal cells: consistent expression of cadherin-11 in osteoblast lineage. *J Bone Miner Res*. 2001;16(2):260-269.
42. Sternberg J, Wankell M, Subramaniam VN, Hebbard LW. The functional roles of T-cadherin in mammalian biology. *Aims Mol Sci*. 2017;4(1):62-81.
43. Philippova M, Joshi MB, Pfaff D, et al. T-cadherin attenuates insulin-dependent signalling, eNOS activation, and angiogenesis in vascular endothelial cells. *Cardiovasc Res*. 2012;93(3):498-507.
44. Philippova M, Ivanov D, Joshi MB, et al. Identification of proteins associating with glycosylphosphatidylinositol- anchored T-cadherin on the surface of vascular endothelial cells: role for Grp78/BiP in T-cadherin-dependent cell survival. *Mol Cell Biol*. 2008;28(12):4004-4017.
45. Ivanov D, Philippova M, Antropova J, et al. Expression of cell adhesion molecule T-cadherin in the human vasculature. *Histochem Cell Biol*. 2001;115(3):231-242.
46. Kuzmenko YS, Kern F, Bochkov VN, Tkachuk VA, Resink TJ. Density- and proliferation status-dependent expression of T-cadherin, a novel lipoprotein-binding glycoprotein: a function in negative regulation of smooth muscle cell growth? *FEBS Lett*. 1998;434(1-2):183-187.
47. Kudrjashova E, Bashtrikov P, Bochkov V, et al. Expression of adhesion molecule T-cadherin is increased during neointima formation in experimental restenosis. *Histochem Cell Biol*. 2002;118(4):281-290.
48. Pfaff D, Schoenenberger AW, Dasen B, Erne P, Resink TJ, Philippova M. Plasma T-cadherin negatively associates with coronary lesion severity and acute coronary syndrome. *Eur Heart J Acute Cardiovasc Care*. 2015;4(5):410-418.
49. Matsuda K, Fujishima Y, Maeda N, et al. Positive feedback regulation between adiponectin and T-cadherin impacts adiponectin levels in tissue and plasma of male mice. *Endocrinology*. 2015;156(3):934-946.
50. Göddeke S, Knebel B, Fahlbusch P, et al. CDH13 abundance interferes with adipocyte differentiation and is a novel biomarker for adipose tissue health. *Int J Obes (Lond)*. 2018;42(5):1039-1050.
51. Fukuda S, Kita S, Obata Y, et al. The unique prodomain of T-cadherin plays a key role in adiponectin binding with the essential extracellular cadherin repeats 1 and 2. *J Biol Chem*. 2017;292(19):7840-7849.
52. Guerrero J, Pigeot S, Müller J, Schaefer DJ, Martin I, Scherberich A. Fractionated human adipose tissue as a native biomaterial for the generation of a bone organ by endochondral ossification. *Acta Biomater*. 2018;77:142-154.
53. Bourgine PE, Klein T, Paczulla AM, et al. *In vitro* biomimetic engineering of a human hematopoietic niche with functional properties. *Proc Natl Acad Sci U S A*. 2018;115(25):E5688-E5695.
54. Schneider CA, Rasband WS, Eliceiri KW. NIH Image to ImageJ: 25 years of image analysis. *Nat Methods*. 2012;9(7):671-675.
55. Doube M, Kłosowski MM, Arganda-Carreras I, et al. BoneJ: Free and extensible bone image analysis in ImageJ. *Bone*. 2010;47(6):1076-1079.
56. Sheets KG, Jun B, Zhou Y, et al. Microglial ramification and redistribution concomitant with the attenuation of choroidal neovascularization by neuroprotectin D1. *Mol Vis*. 2013;19:1747-1759.
57. Bourgine P, Le Magnen C, Pigeot S, Geurts J, Scherberich A, Martin I. Combination of immortalization and inducible death strategies to generate a human mesenchymal stromal cell line with controlled survival. *Stem Cell Res*. 2014;12(2):584-598.
58. Barbero A, Ploegert S, Heberer M, Martin I. Plasticity of clonal populations of dedifferentiated adult human articular chondrocytes. *Arthritis Rheum*. 2003;48(5):1315-1325.
59. Jaiswal N, Haynesworth SE, Caplan AI, Bruder SP. Osteogenic differentiation of purified, culture-expanded human mesenchymal stem cells *in vitro*. *J Cell Biochem*. 1997;64(2):295-312.
60. Jakob M, Démarteau O, Schäfer D, et al. Specific growth factors during the expansion and redifferentiation of adult human articular chondrocytes enhance chondrogenesis and cartilaginous tissue formation *in vitro*. *J Cell Biochem*. 2001;81(2):368-377.
61. Peng Q, Alipour H, Porsborg S, Fink T, Zachar V. Evolution of ASC immunophenotypical subsets during expansion in vitro. *Int J Mol Sci*. 2020;21(4):1408.
62. Yang S, Liu H, Liu Y, Liu L, Zhang W, Luo E. Effect of adiponectin secreted from adipose-derived stem cells on bone-fat balance and bone defect healing. *J Tissue Eng Regen Med*. 2019;13(11):2055-2066.
63. Amend SR, Uluckan O, Hurchla M, et al. Thrombospondin-1 regulates bone homeostasis through effects on bone matrix integrity and nitric oxide signaling in osteoclasts. *J Bone Miner Res*. 2015;30(1):106-115.
64. Rico-Llanos GA, Becerra J, Visser R. Insulin-like growth factor-1 (IGF-1) enhances the osteogenic activity of bone morphogenetic protein-6 (BMP-6) *in vitro* and in vivo, and together have a stronger osteogenic effect than when IGF-1 is combined with BMP-2. *J Biomed Mater Res A*. 2017;105(7):1867-1875.
65. Blache U, Vallmajo-Martin Q, Horton ER, et al. Notch-inducing hydrogels reveal a perivascular switch of mesenchymal stem cell fate. *EMBO Rep*. 2018;19(8):e45964.
66. Wu M, Chen G, Li YP. TGF-β and BMP signaling in osteoblast, skeletal development, and bone formation, homeostasis and disease. *Bone Res*. 2016;4:16009.

67. Lin GL, Hankenson KD. Integration of BMP, Wnt, and notch signaling pathways in osteoblast differentiation. *J Cell Biochem*. 2011;112(12):3491-3501.
68. Rahman MS, Akhtar N, Jamil HM, Banik RS, Asaduzzaman SM. TGF-β/BMP signaling and other molecular events: regulation of osteoblastogenesis and bone formation. *Bone Res*. 2015;3:15005.
69. Colnot C. Cellular and molecular interactions regulating skeletogenesis. *J Cell Biochem*. 2005;95(4):688-697.
70. Zhou J, Wei F, Ma Y. Inhibiting PPARγ by erythropoietin while upregulating TAZ by IGF1 synergistically promote osteogenic differentiation of mesenchymal stem cells. *Biochem Biophys Res Commun*. 2016;478(1):349-355.
71. Kirk B, Feehan J, Lombardi G, Duque G. Muscle, bone, and fat crosstalk: the biological role of myokines, osteokines, and adipokines. *Curr Osteoporos Rep*. 2020;18(4):388-400.
72. Carano RA, Filvaroff EH. Angiogenesis and bone repair. *Drug Discov Today*. 2003;8(21):980-989.
73. Jain RK. Molecular regulation of vessel maturation. *Nat Med*. 2003;9(6):685-693.
74. Hankenson KD, Dishowitz M, Gray C, Schenker M. Angiogenesis in bone regeneration. *Injury*. 2011;42(6):556-561.
75. Kim KI, Park S, Im GI. Osteogenic differentiation and angiogenesis with cocultured adipose-derived stromal cells and bone marrow stromal cells. *Biomaterials*. 2014;35(17):4792-4804.
76. Cai X, Xie J, Yao Y, et al. Angiogenesis in a 3D model containing adipose tissue stem cells and endothelial cells is mediated by canonical Wnt signaling. *Bone Res*. 2017;5:17048.
77. Wang DS, Miura M, Demura H, Sato K. Anabolic effects of 1,25-dihydroxyvitamin D3 on osteoblasts are enhanced by vascular endothelial growth factor produced by osteoblasts and by growth factors produced by endothelial cells. *Endocrinology*. 1997;138(7):2953-2962.
78. Deckers MM, van Bezooijen RL, van der Horst G, et al. Bone morphogenetic proteins stimulate angiogenesis through osteoblast-derived vascular endothelial growth factor A. *Endocrinology*. 2002;143(4):1545-1553.
79. Clark D, Wang X, Chang S, Czajka-Jakubowska A, Clarkson BH, Liu J. VEGF promotes osteogenic differentiation of ASCs on ordered fluorapatite surfaces. *J Biomed Mater Res A*. 2015; 103(2):639-645.
80. Seebach C, Henrich D, Kähling C, et al. Endothelial progenitor cells and mesenchymal stem cells seeded onto beta-TCP granules enhance early vascularization and bone healing in a critical-sized bone defect in rats. *Tissue Eng Part A*. 2010;16(6):1961-1970.
81. Sahar DE, Walker JA, Wang HT, et al. Effect of endothelial differentiated adipose-derived stem cells on vascularity and osteogenesis in poly(D,L-lactide) scaffolds in vivo. *J Craniofac Surg*. 2012;23(3):913-918.
82. Fuchs S, Hofmann A, Kirkpatrick C. Microvessel-like structures from outgrowth endothelial cells from human peripheral blood in 2-dimensional and 3-dimensional co-cultures with osteoblastic lineage cells. *Tissue Eng*. 2007;13(10):2577-2588.
83. Stahl A, Wenger A, Weber H, Stark GB, Augustin HG, Finkenzeller G. Bi-directional cell contact-dependent regulation of gene expression between endothelial cells and osteoblasts in a three-dimensional spheroidal coculture model. *Biochem Biophys Res Commun*. 2004;322(2):684-692.
84. Villars F, Bordenave L, Bareille R, Amédée J. Effect of human endothelial cells on human bone marrow stromal cell phenotype: role of VEGF? *J Cell Biochem*. 2000;79(4):672-685.
85. Villars F, Guillotin B, Amédée T, et al. Effect of HUVEC on human osteoprogenitor cell differentiation needs heterotypic gap junction communication. *Am J Physiol Cell Physiol*. 2002;282(4):C775 -C785.
86. Lee CS, Burnsed OA, Raghuram V, Kalisvaart J, Boyan BD, Schwartz Z. Adipose stem cells can secrete angiogenic factors that inhibit hyaline cartilage regeneration. *Stem Cell Res Ther*. 2012;3(4):35.
87. Bakker AH, Nijhuis J, Buurman WA, van Dielen FM, Greve JW. Low number of omental preadipocytes with high leptin and low adiponectin secretion is associated with high fasting plasma glucose levels in obese subjects. *Diabetes Obes Metab*. 2006;8(5):585-588.
88. Ye J, Gimble JM. Regulation of stem cell differentiation in adipose tissue by chronic inflammation. *Clin Exp Pharmacol Physiol*. 2011;38(12):872-878.
89. Fischer LJ, McIlhenny S, Tulenko T, et al. Endothelial differentiation of adipose-derived stem cells: effects of endothelial cell growth supplement and shear force. *J Surg Res*. 2009;152(1):157-166.
90. Shaked Y, Ciarrocchi A, Franco M, et al. Therapy-induced acute recruitment of circulating endothelial progenitor cells to tumors. *Science*. 2006;313(5794):1785-1787.
91. Tran KV, Gealekman O, Frontini A, et al. The vascular endothelium of the adipose tissue gives rise to both white and brown fat cells. *Cell Metab*. 2012;15(2):222-229.
92. Curat CA, Miranville A, Sengenès C, et al. From blood monocytes to adipose tissue-resident macrophages: induction of diapedesis by human mature adipocytes. *Diabetes*. 2004;53(5):1285-1292.
93. Navarro A, Marín S, Riol N, Carbonell-Uberos F, Miñana MD. Human adipose tissue-resident monocytes exhibit an endothelial-like phenotype and display angiogenic properties. *Stem Cell Res Ther* 2014;5(2):50.